Microsphere whispering-gallery-mode laser using HgTe quantum dots

S. I. Shopova, G. Farca, and A. T. Rosenberger[a)]
Department of Physics, Oklahoma State University, Stillwater, Oklahoma 74078-3072

W. M. S. Wickramanayake and N. A. Kotov
Department of Chemical Engineering, University of Michigan, Ann Arbor, Michigan 48109

(Received 27 September 2004; accepted 27 October 2004)

Ultralow-threshold continuous-wave lasing is achieved at room temperature in a fused-silica microsphere that is coated with HgTe quantum dots (colloidal nanoparticles). The 830 nm pump input and HgTe microlaser output are efficiently coupled into and out of whispering-gallery modes by tapered fibers. Lasing occurs at wavelengths ranging from 1240 to 1780 nm, depending on the size and composition of the quantum dots (HgCdTe is also used). A linear fit to the data determines the lowest observed threshold pump power to be 0 ± 2 μW. © *2004 American Institute of Physics*. [DOI: 10.1063/1.1841459]

Fused-silica microspheres have been studied extensively over the past several years as high-quality-factor (Q), low-mode-volume optical resonators of wide-ranging applicability. The Q of a resonator mode is defined as the ratio of resonance frequency ν_c to mode linewidth $\Delta\nu$, so high Q values imply narrow linewidths and long cavity lifetimes. A high-Q eigenmode of a microsphere in which light circulates in the equatorial plane, trapped near the surface by total internal reflection, with an integer number of wavelengths along a circumferential trajectory, is a whispering-gallery mode (WGM). Part of the field distribution of a WGM extends outside the sphere; this evanescent component enables interaction with material on the surface or in the surrounding medium. Potential uses of these WGM microresonators range from fundamental studies of cavity quantum electrodynamics to practical applications such as sensors, optical spectrum analyzers, and microlasers. Recently, microspherical lasers employing several different techniques of introducing gain have been demonstrated.[1–5] Also ongoing over the past several years has been concentrated investigation of the strongly size-dependent optical properties of semiconductor quantum dots (or nanoparticles or nanocrystals). In the strong-confinement regime, where the quantum dot is small compared to the electron–hole exciton Bohr radius, the electronic transitions become discrete, and the dots are often referred to as "artificial atoms." By combining the advantages of a microspherical resonator and a quantum-dot gain medium,[6–12] we take another step toward achieving microlasers with ultralow thresholds and high efficiencies.

In this letter we report a microsphere whispering-gallery-mode laser, with a gain medium consisting of HgTe (or HgCdTe) quantum dots on the sphere's surface. In contrast to lasing media based on CdSe nanoparticles,[13] $Hg_{1-x}Cd_xTe$ enables extension of the lasing capabilities to the infrared region and provides the possibility of overcoming certain intrinsic limitations to the realization of quantum-dot lasers. These limitations are related to fast Auger recombination and other depopulation processes.[14] Tapered fibers provide efficient coupling for the optical pump and for the microlaser emission, unlike some previous WGM quantum-dot lasers that used free-space coupling.[7–9] Ultralow-threshold cw operation is observed at room temperature. Our procedures emphasize simplicity and flexibility: we easily fabricate fused-silica microspheres ranging in diameter from 100 to 1000 μm by melting the end of an optical fiber with a hydrogen–oxygen torch; our coating method simplifies control of the surface density of quantum dots deposited on the microsphere; and we have so far produced lasing wavelengths that range from 1240 to 1780 nm by using nanoparticles of different sizes and compositions.

We chose colloidally prepared spherical HgTe nanoparticles for the microlaser's active medium because of their strong room-temperature infrared photoluminescence (quantum efficiency ~50%).[15] Depending on the size distribution and the method of preparation (the size dispersion in a typical batch is about 20%), these nanoparticles can exhibit a broad luminescence spectrum (1200–2000 nm) covering the telecommunication bands.[16] In the present work we used D_2O as a solvent instead of water, in order to reduce the absorption of the surface coating at the long emission wavelengths. A bilayer coating method was used to functionalize the surface of the silica microsphere, in a manner similar to the layer-by-layer method previously used for preparation of both multilayers[17] and (sub)monolayers[18] of semiconductor nanoparticles. First the microsphere was dipped in a 0.5% D_2O solution of poly(dimethyldiallylammonium) chloride (PDDA) to obtain a positively charged layer of polyelectrolyte on the surface. Then the microsphere was dipped in a D_2O solution of negatively charged HgTe nanoparticles long enough to produce approximately 1% of a monolayer, as determined by atomic force microscopy of a coated microsphere. The negative charge of the HgTe nanoparticles originates from the organic stabilizer coating their surfaces, which in this case was thioglycolic acid. The polyelectrolyte macromolecules adjust their coverage on the silica surface to form transparent shells (collars) around the HgTe nanoparticles,[18] reducing photoinduced corrosion and improving their adherence to the microsphere.

Excitation by the evanescent component of the 830 nm pump light coupled into a WGM of the microsphere produces an active medium consisting of 10^6–10^7 quantum dots, each typically 3–4 nm in diameter. The excitation method is illustrated in the schematic of the experimental setup shown in Fig. 1. The pump is coupled into a WGM of

[a)]Electronic mail: atr@okstate.edu

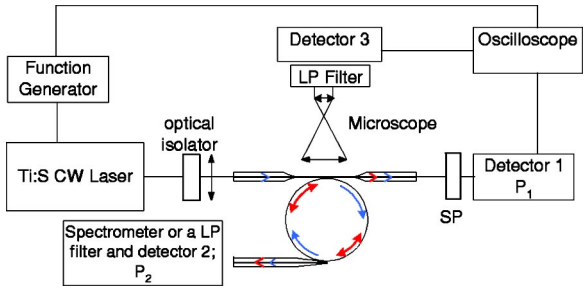

FIG. 1. (Color online) Experimental setup. Light from a frequency-scanned cw Ti:sapphire laser (blue) is launched into a bitapered fiber to excite WGMs of the microsphere and pump the quantum dots, which produce microlaser emission (red). LP and SP denote filters that pass long (>900 nm) and short (<900 nm) wavelengths, respectively.

the microsphere via a biconical tapered fiber having a diameter optimized[19] for efficient coupling of the pump wavelength. Microlaser emission is coupled out either through the pump-coupling fiber or through a second tapered fiber. The second fiber is optimized for coupling at the longer wavelength of the emission and is quite inefficient for outcoupling of the pump wavelength.

Also shown in Fig. 1 is the detection and measurement system. The pump throughput is measured by detector 1, a Si photodiode (Newport 818-SL). Detector 2 is a Ge photodiode (Newport 818-IR) for the microlaser emission. Input–output measurements were made by simultaneous display on the oscilloscope of the signals from detectors 1 and 2. The microscope is actually above the plane of the figure, and looks down on a pole of the sphere. It is used for visual alignment of the couplers; in addition, detector 3 was used to observe the light scattered from the periphery of the sphere. This is either a Si detector for measuring scattered pump light or a Ge detector (with long-pass filter) for observing scattered microlaser emission.

We chose to scan the laser slowly over a small frequency range (1 GHz at a 0.5 Hz repetition rate), rather than trying to stay on a particular pump WGM. This scan rate is slow enough that we can say with confidence that quasi-cw laser emission was observed; the time scale for changes in the emission due to pump scanning is far longer than the cavity or material lifetimes. Scanning the pump gives us an additional means of determining the onset of lasing, as discussed later. To avoid thermal bistability effects we kept the pump power incident on the microsphere lower than a few milliwatts.

Detector 2 in Fig. 1 can be replaced with a scanning monochromator (SpectraPro-300) to determine the microlaser emission wavelengths. These spectral measurements, an example of which is shown in Fig. 2, typically indicate multimode laser operation over a narrow portion of the photoluminescence spectrum. The photoluminescence is measured from a solution of the same batch of nanoparticles, but in a separate experiment. The limited spectrometer resolution (0.1 nm) does not allow us to distinguish individual lasing WGMs. The observed microlaser emission wavelengths, using different batches of nanoparticles having different semiconductor cores but similar organic coatings, are in the 1240–1780 nm range. Longer wavelengths are produced by HgTe and shorter by $Hg_{0.8}Cd_{0.2}Te$. The blueshift of the lasing wavelength for $Hg_{0.8}Cd_{0.2}Te$ is consistent with the increase of absolute energy of the conduction band when Cd

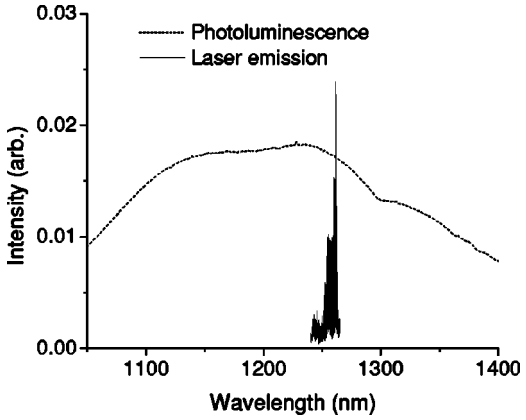

FIG. 2. Broad photoluminescence and narrow laser emission spectra from the same batch of $Hg_{0.8}Cd_{0.2}Te$ nanoparticles prepared in D_2O solution. Similar results are obtained from HgTe nanoparticles.

atoms are added to the crystal lattice, thereby widening the band gap.[20]

Microlaser output power is shown in Fig. 3 as a function of absorbed pump power. Data for two different HgTe-coated microspheres are given. One had a diameter of 650 μm, pump Q of 2×10^6, and lasing Q of about 10^7 (around 1620 nm, estimated from measurements made on the microsphere before coating); a linear fit to the data gives a threshold pump power of $P_{th}=9.41\pm2.35$ μW. The other had a diameter of 950 μm, pump Q of 2×10^7, and lasing Q of about 10^8 (around 1670 nm); the linear fit gives $P_{th}=-0.06\pm2.18$ μW. The latter case suggests a large capture fraction β of spontaneous emission into the lasing WGMs.[10,11] The thresholds and their uncertainties are overestimated, probably by an order of magnitude, because we calculated the absorbed pump power ($\sim$25% of the total input pump power) without accounting for losses due to scattering and to outcoupling via the second fiber. In the future, the experiment will be modified to allow more precise measurements of these loss mechanisms, especially surface scattering, which appears to be by far the dominant pump loss. The measured slope efficiencies of $2-4\times10^{-4}$ are likewise underestimated by at least an order of magnitude. The overestimate of pump absorption also contributes to this, as do

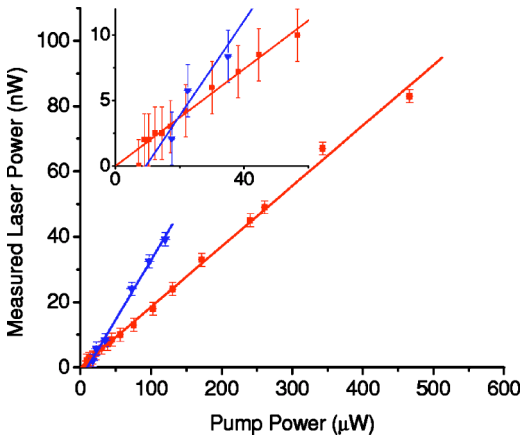

FIG. 3. (Color online) Measured microlaser output (one fiber, one direction) vs estimated absorbed pump power. The inset shows the region near the origin. Triangles (blue): microsphere diameter 650 μm, threshold pump power 9.4 μW. Squares (red): diameter 950 μm, zero threshold. The lines are linear fits to the data.

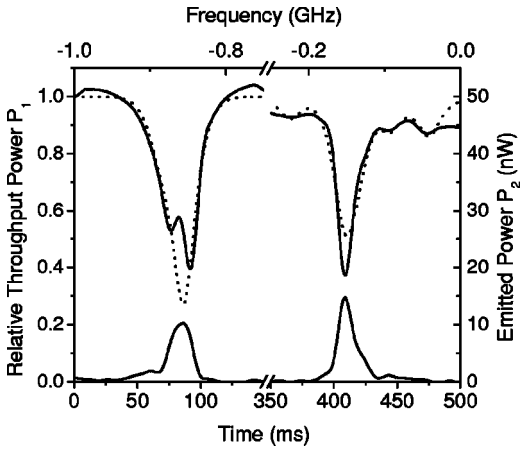

FIG. 4. Effect of lasing on pump throughput. The upper oscilloscope traces are pump throughput (left axis) and the lower are microlaser output (right axis), recorded simultaneously as the pump scans in frequency. The time scale is shown at the bottom and the relative pump frequency is shown at the top. Left: undercoupled pump mode; right: overcoupled. The dotted curves are fits showing approximately what the pump dips would look like in the absence of lasing-enhanced absorption.

measurement of just a fraction of the output power (one fiber, one direction) and water absorption of the microlaser emission. (With time, the D_2O in the coating is replaced by water; rinsing with D_2O after several days of use can increase the microlaser power by more than a factor of 2.) We also find that either pump polarization, TE (tangential) or TM (radial), can produce laser emission of both polarizations.

The laser threshold can also be determined from the effect that lasing has on the pump resonances (throughput dips, Fig. 4). When microlaser emission occurs, the pump absorption increases due to lasing-enhanced recombination. When the pump WGM is overcoupled (coupling loss greater than intrinsic loss), this increase in its intrinsic loss drives the system closer to critical coupling, increasing the dip depth. This was observed for the lower-threshold laser of Fig. 3, where the dip got 2.5% deeper as the absorbed pump power increased from 7.2 to 470 μW. For an undercoupled WGM, the pump dip depth decreases when a laser mode turns on. Examples of both undercoupled and overcoupled pump modes are shown in Fig. 4. Undercoupled modes, in particular, can provide a convenient alternative way to measure the threshold.

In conclusion, lasing from HgTe and HgCdTe nanoparticles attached to the surface of a microsphere was investigated. The ability to choose the emission wavelength by changing the stoichiometry and the size of the quantum dots was demonstrated. Ultralow-threshold lasing was observed, with a probable upper limit of 200 nW on threshold absorbed pump power and probable slope efficiency of nearly 1%. The onset of lasing was also determined through related changes in the pump throughput that depend on the pump coupling. These microlasers have potential applications in telecommunications and in chemical sensing.

This work was supported by the Oklahoma Center for the Advancement of Science and Technology under Project No. AR012-064 and by the National Science Foundation under Award No. ECS-0115442. The authors thank J. P. Rezac, A. Naweed, D. K. Bandy, and M. J. Humphrey for assistance, and M. Lucas for instrument construction.

[1]V. Sandoghdar, F. Treussart, J. Hare, V. Lefèvre-Seguin, J.-M. Raimond, and S. Haroche, Phys. Rev. A **54**, R1777 (1996).
[2]M. Cai, O. Painter, K. J. Vahala, and P. C. Sercel, Opt. Lett. **25**, 1430 (2000).
[3]F. Lissillour, D. Messager, G. Stéphan, and P. Féron, Opt. Lett. **26**, 1051 (2001).
[4]L. Yang and K. J. Vahala, Opt. Lett. **28**, 592 (2003).
[5]K. An and H.-J. Moon, J. Phys. Soc. Jpn. **72**, 773 (2003).
[6]X. Fan, P. Palinginis, S. Lacey, H. Wang, and M. C. Lonergan, Opt. Lett. **25**, 1600 (2000).
[7]M. V. Artemyev, U. Woggon, R. Wannemacher, H. Jaschinski, and W. Langbein, Nano Lett. **1**, 309 (2001).
[8]S. Lu, D. Jiang, R. Jia, L. An, L. Bian, X. Liang, B. Ma, and B. Sun, J. Phys.: Condens. Matter **14**, 6395 (2002).
[9]Y. P. Rakovich, L. Yang, E. M. McCabe, J. F. Donegan, T. Perova, A. Moore, N. Gaponik, and A. Rogach, Semicond. Sci. Technol. **18**, 914 (2003).
[10]M. Pelton and Y. Yamamoto, Phys. Rev. A **59**, 2418 (1999).
[11]O. Benson and Y. Yamamoto, Phys. Rev. A **59**, 4756 (1999).
[12]A. N. Oraevskii, M. O. Scully, and V. L. Velichanskii, Kvantovaya Elektron. (Moscow) **25**, 211 (1998) [Quantum Electron. **28**, 203 (1998)].
[13]H.-J. Eisler, V. C. Sundar, M. G. Bawendi, M. Walsh, H. I. Smith, and V. Klimov, Appl. Phys. Lett. **80**, 4614 (2002).
[14]V. I. Klimov, Ch. J. Schwarz, D. W. McBranch, C. A. Leatherdale, and M. G. Bawendi, Phys. Rev. B **60**, R2177 (1999).
[15]A. Rogach, S. Kershaw, M. Burt, M. Harrison, A. Kornowski, A. Eychmuller, and H. Weller, Adv. Mater. (Weinheim, Ger.) **11**, 552 (1999).
[16]A. L. Rogach, D. S. Koktysh, M. Harrison, and N. A. Kotov, Chem. Mater. **12**, 1526 (2000).
[17]N. A. Kotov, MRS Bull. **26**, 992 (2001).
[18]Z. Tang, Y. Wang, and N. A. Kotov, Langmuir **18**, 7035 (2002).
[19]J. C. Knight, G. Cheung, F. Jacques, and T. A. Birks, Opt. Lett. **22**, 1129 (1997).
[20]A. L. Rogach, M. T. Harrison, S. V. Kershaw, A. Kornowski, M. G. Burt, A. Eychmüller, and H. Weller, Phys. Status Solidi B **224**, 153 (2001); L. Fradkin, L. Langof, E. Lifshitz, A. Rogach, N. Gaponik, H. Weller, and A. Eychmüller, ChemPhysChem **4**, 1203 (2003).